ELSEVIER

Journal of Nuclear Materials 290–293 (2001) 663–667

journal of nuclear materials

www.elsevier.nl/locate/jnucmat

Investigations on density and temperature asymmetries due to drift motions in the boundary layer of TEXTOR-94

M. Lehnen [a,*], M. Brix [a], H. Gerhauser [a], B. Schweer [a], R. Zagórski [b]

[a] *Institut für Plasmaphysik, Forschungszentrum Jülich GmbH, EURATOM Association, Trilateral Euregio Cluster, D-52425 Jülich, Germany*

[b] *Institute of Plasma Physics and Laser Microfusion, Hery Street 23, PL-00-908 Warsaw, Poland*

Abstract

Electron densities and temperatures in the plasma edge have been measured by means of the helium beam diagnostic. Furthermore, the charge exchange signal driven by the thermal helium beam atoms has been used to measure the poloidal velocities of C^{6+} ions. Asymmetries in the radial profiles of the edge parameters have been found. For further analysis of the physical mechanisms, calculations have been performed with the 2D boundary layer code TECXY. Experimental and modeled results are compared. The influence of the line averaged electron density and the heating power on the electron density and temperature ratios between low field side (LFS) and high field side (HFS) inside the scrape off layer (SOL) is shown. Not only drift motions but also other effects such as recycling at the limiters have an important influence on the spatial structure of the plasma parameters in the SOL.

Keywords: Edge plasma; Drift; SOL; *B*-field reversals; Helium; TEXTOR

1. Introduction

Asymmetries of plasma parameters in the boundary layer of tokamak plasmas have been found in various machines with limiter or divertor configuration (for an overview see, e.g., [1]). Different densities and temperatures at both sides of the limiter or divertor may lead to an asymmetric heat load which has influence on erosion and deposition. Analytical models have been applied to study the influence of drifts [2]. For a detailed analysis of the measurements 2D code calculations including drift terms are necessary.

Former measurements on TEXTOR with thermal lithium beams have already shown asymmetric density profiles [3] at both sides of the toroidal belt limiter. The helium beam diagnostics allows to measure simultaneously density and temperature profiles over a larger radial range even in high density discharges. Furthermore, the injection of He atoms provides an active charge exchange diagnostic for the local determination of ion velocities. In many publications, the presented plasma edge parameters were measured in ohmic heated discharges. The discussed results in this paper were derived from discharges with neutral beam injection.

2. Diagnostics

TEXTOR-94 is a limiter tokamak with a pumped toroidal belt limiter. The poloidal cross-section is circular. The minor radius of the machine is 0.46 m, the major radius 1.75 m. All discharges presented here were performed with $B_\phi = 2.25$ T and $I_P = 350$ kA. The helium beam diagnostic has been used to measure electron temperatures and densities at the low field side (LFS) and high field side (HFS) of the tokamak. A detailed description of the method is given in [4]. The good radial resolution of this diagnostic (less than 2 mm) is necessary to investigate radial structures in the boundary

* Corresponding author. Tel.: +49-2461 61 6611; fax: +49-2461 61 3331.

E-mail address: m.lehnen@fz-juelich.de (M. Lehnen).

0022-3115/01/$ - see front matter
PII: S0022-3115(00)00521-3

layer of TEXTOR-94. The accuracy of the absolute values is determined by a systematic error due to the uncertainties in the data used in the collisional-radiative model, and a random error produced by the measurement itself. The overall error has been estimated to be within ±30% for the temperature and ±20% for the density measurements. The relative error when comparing measurements at, e.g., different positions is lower. In this case, the main contribution is the background radiation originating from impurities and recycled helium. The background has been measured within the flattop phase of the discharge before helium was injected. The helium flux into the vessel is about 6×10^{18} atoms/s when using both diagnostics (LFS and HFS). This leads to a maximum He to D flux ratio at the toroidal belt limiter ALT-II of about 1%.

A new method is the application of a thermal helium beam for charge exchange recombination spectroscopy (CXRS). The aim of these measurements is to obtain radial profiles of the poloidal plasma rotation velocity extracted from the Doppler shift of the C VI line at $\lambda = 529$ nm. The expected velocities are in a range of a few kilometers per second. A high resolution spectrometer with $\lambda/\Delta\lambda = 1.5 \times 10^5$ allows to resolve velocities down to 100 m/s. The observation system consists of six lightguides collecting light from the LFS within a radial and toroidal range of 5 mm (see Fig. 1).

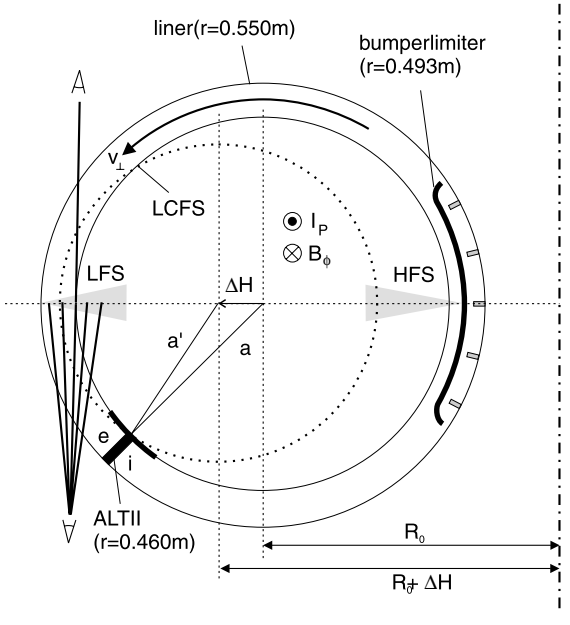

Fig. 1. Poloidal geometry in TEXTOR-94. A shift of the plasma column towards the LFS leads to a smaller plasma radius a. The position of the LCFS is shifted about $1.7 \times \Delta H$ at the HFS, whereas the shift at the LFS is $0.3 \times \Delta H$. The observation geometry for the CXRS is outlined. The e- and i-side of the limiter is indicated for normal field orientation (e,i).

One of these lightguides is situated opposite to the others, so that the opposite Doppler shift allows the determination of the unshifted wavelength. The good radial resolution is possible due to the width of the helium beam of only 60 mm in contrast to the minor plasma radius.

The comparison of plasma parameters at different positions in the boundary layer is very sensitive to the plasma position. In particular, the plasma parameters at the HFS are very sensitive to a plasma shift, whereas the position of the LCFS at the LFS is almost fixed due to the ALT II (Fig. 1). The position of the plasma column has been controlled with the HCN interferometer by adjusting the line integrated density at $R - R_0 = \pm 0.3$ m [5]. With a variation of the plasma pressure the Shafranov shift changes the position of the last closed flux surface (LCFS). We assume that the shift of the flux surfaces over the normalized plasma radius ϱ varies like $\delta(\varrho) = \delta_0(1 - \varrho^2)$, with δ_0 being the Shafranov shift in the center. The density profile can also be approximated by a parabolic function. The integration along the line of sight of the interferometer gives us then the shift of the LCFS $\Delta H \approx -0.38 \times \delta_0$. The Shafranov shift is connected to the poloidal beta by δ_0 [mm] $\approx 23 + 60 \times \beta_p$, which has been found from numerical equilibrium calculations [6]. The Shafranov shift has of course also influence on the radial gradients of the plasma parameters.

3. Drift effects

The dominant drift motions in the boundary layer arise from electric fields and pressure gradients perpendicular to the magnetic field. The velocities of the perpendicular drifts $v_\perp$ ($\mathbf{v}_\perp \perp \mathbf{v}_r \perp \mathbf{B}$) are in the range of 1–5 km/s, estimated from typical edge plasma parameters in TEXTOR-94. The radial drift velocities v_r are much lower, in the order of 20 m/s, but increase in the vicinity of the limiter. In discharges with normal orientation of the magnetic field, the perpendicular drift flow in the scrape off layer (SOL) is directed towards the electron drift side (e-side) of the toroidal limiter and away from the limiter's ion drift side (i-side). The direction of the magnetic field, the plasma current and the drift flow is indicated in Fig. 1. The perpendicular drifts have influence on the parallel velocity due to the boundary condition (Bohm criterion) at the limiter [7]. The poloidal velocity is fixed to the projection of the sound speed $v_\theta = \pm c_s B_\theta/(B_\theta + B_\phi)$ leading to a parallel flow of $v_\parallel = \pm c_s - v_\perp B_\phi/B_\theta$ at the e-side/i-side of the limiter [8]. Due to the reduced parallel flow, the electron density is expected to be higher at the e-side.

Fig. 2 shows measured density profiles at the LFS and HFS of neutral beam heated discharges ($P_{NBI} = 1.3$ MW) for different line averaged densities. With in-

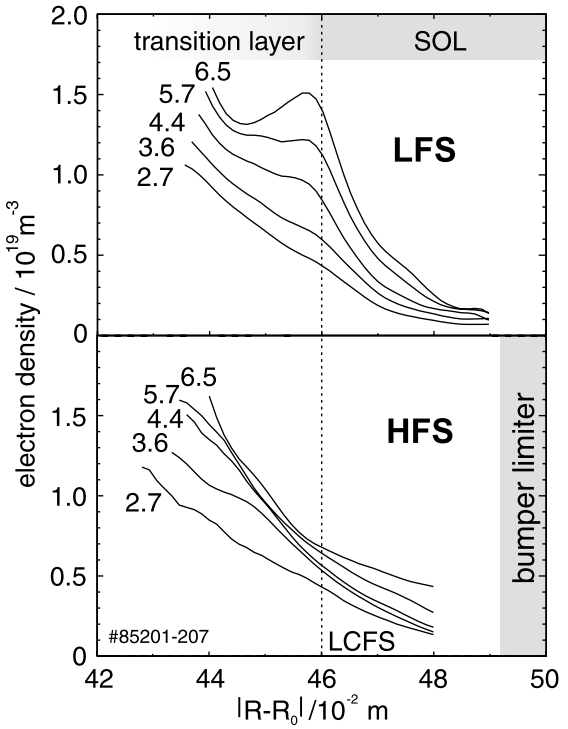

Fig. 2. Helium beam measurements: density profiles at LFS and HFS. The numbers refer to the line averaged density $\bar{n}_e/10^{19}$ m^{-3}.

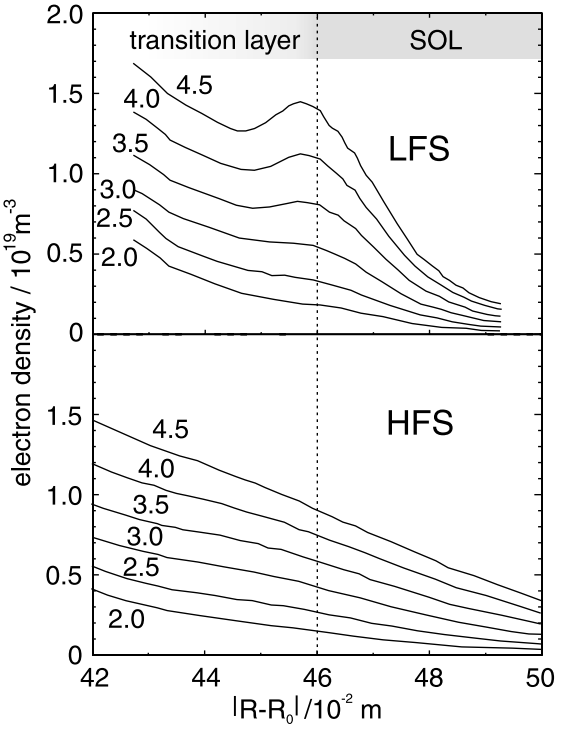

Fig. 3. TECXY: density profiles at LFS and HFS. The numbers refer to the particle input into the boundary plasma $\Gamma_{in}/10^{21}$ s^{-1}.

creasing density, a shoulder with a local minimum is developing, whereas at the HFS this shoulder is not visible. The observation can be explained by drift effects together with the recycling behaviour at the toroidal belt limiter. The perpendicular drift leads to a particle transport towards the e-side of the limiter (near to the LFS) in the SOL and away from the e-side in the transition layer. Parallel electric fields and pressure gradients in the vicinity of the limiter drive a radial drift. The drift at the e-side is directed towards the LCFS in the SOL and enhances the development of the shoulder [9]. In low density discharges the shoulder is less pronounced or even vanished. Calculations with the 2D fluid code TECXY [7,8], which includes the drift motions are given in Fig. 3. In these calculations, not only the input flux into the boundary layer has been changed, but also the recycling factor has been increased from $R = 0.5$ at low density to $R = 0.83$ for the high density case. In this case, R is the fraction of neutrals, which are ionized in the boundary layer ($|R - R_0| = 0.55$ to 0.42 m). The good agreement with the measured data confirms the strong influence of drifts and recycling on the radial profiles. It has been shown [8] that the shoulder vanishes when the drift terms in the model are neglected. At the HFS some discrepancy exists in the steepness of the gradients which might be due to asymmetric transport coefficients. Also the influence of the bumper limiter is not included in the model.

We have performed discharges with inverted toroidal and poloidal magnetic field orientation in order to change the direction of the drift motions. In Fig. 4, profiles of the ratios of the plasma parameters (electron density, temperature and pressure) for normal and inverted configuration are shown for the LFS position. The measured pressure is higher for the normal case than for the inverted one, this is in qualitative agreement with the calculations from TECXY. The measured density and temperature ratios in the SOL are as in the calculations above 1, even though there is a quantitative discrepancy. The behaviour in the transition layer could not be modelled. The density ratio drops below 1 and the temperature ratio rises up to 1.2. A possible explanation for this discrepancy is the influence of impurities. In the inverted case the carbon flux at the toroidal limiter was increased by a factor of 2. This leads to a more pronounced cooling effect and an increase in density especially in the first 40 mm inside the LCFS where the carbon starting from the limiter is ionized up to C^{3+} [10].

Fig. 5 shows the measured poloidal velocities of the C^{6+} ions for both cases (normal/inverted) in comparison to the modelled ones for deuterium. The poloidal velocity consists of two contributions: $v_\theta = v_\perp \cos\alpha +$

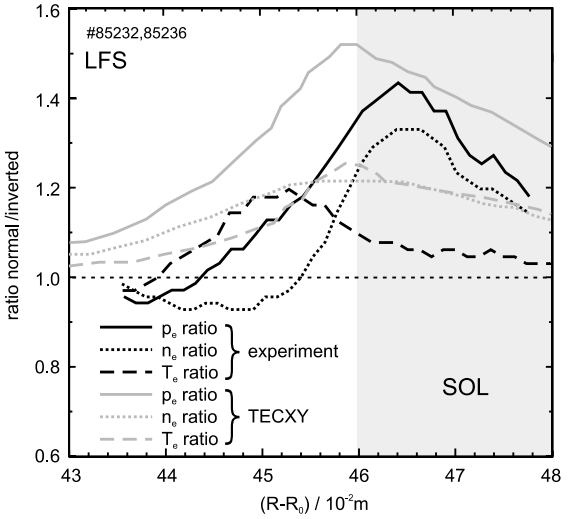

Fig. 4. Electron density, temperature and pressure ratio between normal and inverted configuration at the LFS.

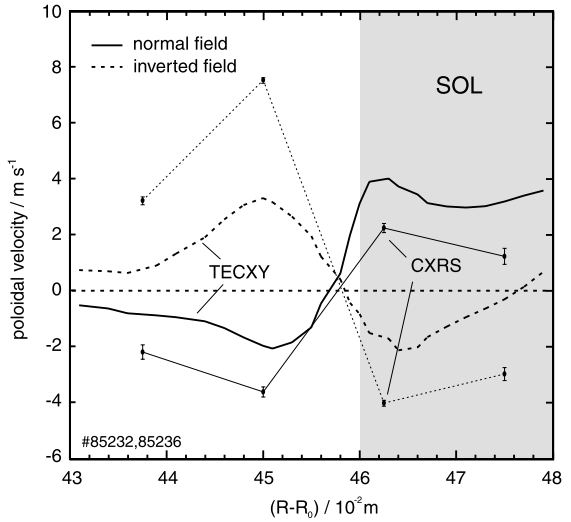

Fig. 5. Poloidal velocity of C^{6+} measured with the helium beam diagnostic at the LFS in a medium density discharge ($\bar{n}_e = 3.5 \times 10^{19}$ m^{-3}) with NBI.

$v_\parallel \sin \alpha$, where α is the inclination angle of the field lines ranging from 3° to 7° depending on the safety factor q, so that the contribution from the parallel velocity is at maximum 12%. The measured and modelled velocities show the same qualitative behaviour, though two different species are compared. Since the electric field in the SOL is expected to originate from the temperature dependence of the sheath potential, the electric drift is the same for both species. The diamagnetic drift is charge dependent and should be smaller for the C^{6+} ions. However, this might be cancelled to some extend by the density gradient. Measurements of the density in ohmic discharges have shown that the radial gradient for C^{6+} in the SOL is much steeper than the density gradient for the electrons [11]. The radial electric field inside the LCFS has been calculated by the TECXY code from a presumed drift velocity. In [12], it is shown that the electric field can also be found self-consistent from the ambipolarity constraint, leading to comparable results. The measurement of the velocities confirms the existence of two poloidally rotating layers, one in the SOL towards the electron side of the limiter and one in the transition zone into the opposite direction. The flows reverse, when the magnetic fields are inverted. The change in the particle flow in the SOL leads to the pressure difference in Fig. 4.

4. Parameter scans

Fig. 6 shows the density ratio between HFS and LFS in the SOL as a function of the line averaged density. The density ratio decreases from about 1.6 in low density discharges to 0.8 in the high density discharges. The temperature ratio also shows a slight dependence on the density. Since the temperature gradients flatten with increasing density, the perpendicular drift velocities in the SOL decrease from 5 to 1 km/s (electric and diamagnetic drifts are deduced from measured temperature and pressure gradients). If the drift motions would be the only mechanism, the density ratio HFS/LFS is then expected to increase. The ratio of the neutral flux between the main limiter and the bumper limiter depends also strongly on the line averaged density. In particular, at low densities the bumper limiter is a non-negligible

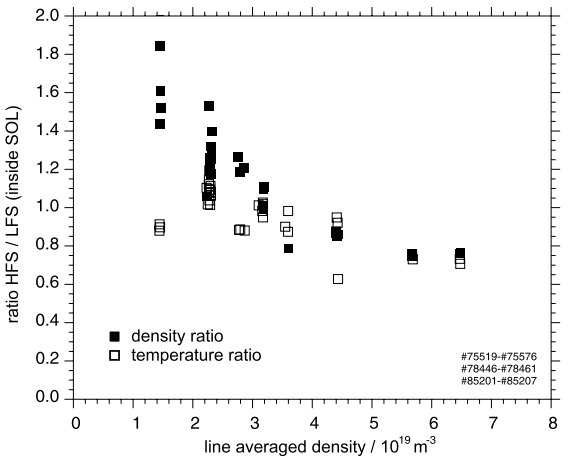

Fig. 6. Density ratio between HFS and LFS inside the SOL ($|R - R_0| = a + 10$ mm) for different line averaged densities. The discharges were NBI heated with co-injection and beam power of $P_{NBI} = 1.3$ MW.

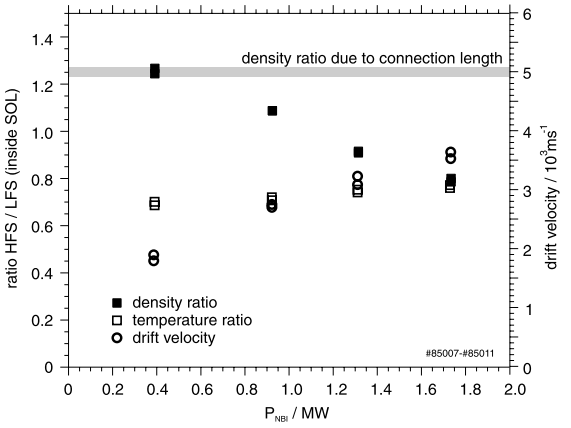

Fig. 7. Influence of the heating power on the density and temperature ratio between HFS and LFS inside the SOL ($|R - R_0| = a + 10$ mm). The line averaged density for these discharges is $\bar{n}_e = 4.5 \times 10^{18}$ m^{-3}. Co- and counter-injection has been used with a power difference of $\Delta P_{NBI} \approx 0.4$ MW to keep the toroidal rotation constant. The grey line indicates the density ratio resulting from the different connection length of the two poloidal positions.

neutral source, which might lead to the large density ratio up to 1.6. In the high density case the recycling at the main limiter clearly dominates.

In Fig. 7, the density and temperature ratios HFS/LFS in the SOL are plotted versus the power injected by the neutral heating beam. The density ratio drops with increasing power. Since the drift velocity increases with the injected power (from 1.8 to 3.7 km/s) this behaviour can be understood when the drift is considered as the driving mechanism. The temperature ratio increases with the input power.

Although the model calculations reproduce the measured radial structure, there is a discrepancy between model and experiment concerning the poloidal structure, namely, the density and temperature ratios between HFS and LFS. But still some mechanism, which might induce the measured behaviour are not included in TECXY. The recycling at the bumper limiter, e.g., can make a non-negligible contribution. Additionally the shift of the plasma position may influence the structure of the SOL.

5. Summary

We have shown that the shape of the radial electron density profile is strongly influenced by drift motions and recycling properties. The effect of drift motions has been made visible by comparing radial profiles of the plasma parameters at the LFS for normal and inverted magnetic fields. The observed effects could be clearly related to a poloidal plasma rotation. From the measurements of electron density and temperature at the HFS and the LFS it has been shown that asymmetries between these two poloidal positions exist and are influenced by the line averaged density and the heating power. The density ratio HFS/LFS is very sensitive to the line averaged density, which cannot be explained by drifts only. Particle sources may play a dominant role. For further investigations measurements of the neutral source distribution would be valuable. Also the influence of the asymmetric heating, the bumper limiter and asymmetric transport should be studied with the model code.

References

[1] C.S. Pitcher, P.C. Stangeby, Plasma Phys. Control. Fus. 39 (1997) 779.
[2] P.C. Stangeby, A.V. Chankin, Nucl. Fus. 36 (1996) 839.
[3] U. Samm et al., Nucl. Fus. 31 (1991) 1386.
[4] B. Schweer, M. Brix, M. Lehnen, J. Nucl. Mater. 266–269 (1999) 673.
[5] H. Soltwisch, Nucl. Fus. 23 (1983) 1681.
[6] H. Soltwisch, Report Jul-2339, 1990, ISSN 0366–0885.
[7] H. Gerhauser, H.J. Claassen, J. Nucl. Mater. 176,177 (1990) 721.
[8] H. Gerhauser, R. Zagórski, H.A. Claassen, M. Lehnen, Contrib. Plasma Phys. 40 (2000) 309.
[9] M. Lehnen et al., in: Proceedings of the 26th EPS Conference on Controlled Fusion and Plasma Physics, Maastricht, Netherlands 1999, p. P2.034.
[10] M.Z. Tokar', Plasma Phys. Control. Fus. 36 (1994) 1819.
[11] R.P. Schorn et al., Appl. Phys. B 52 (1991) 71.
[12] H. Gerhauser, R. Zagórski, H.A. Claassen, M. Lehnen, these Proceedings.